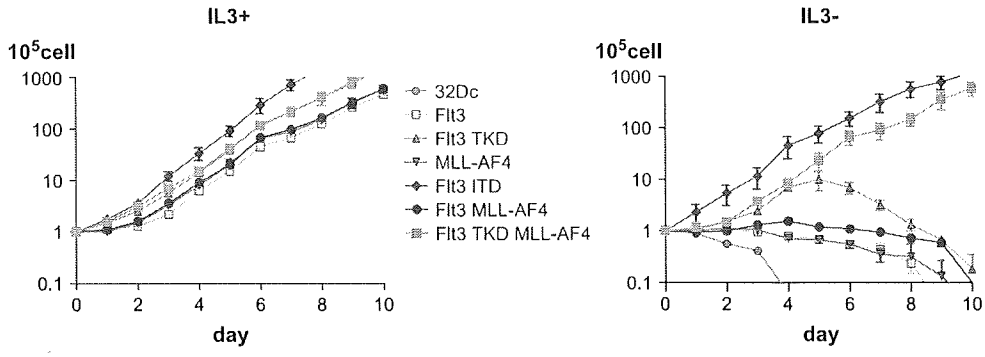


**Figure 2.** Non–interleukin-3 (IL-3)–dependent growth of 32Dc cells expressing either Fms-like tyrosine kinase 3 (Flt3) internal tandem duplication (ITD) or Flt3-TKD + MLL-AF4. In the presence (left figure) or absence (right figure) of interleukin-3 (IL-3), $1 \times 10^5$ cells were cultured to examine cell proliferation. Until 10 days after the start of culture, dead cells were removed using the trypan blue assay, and cell growth curves were prepared based on the number of viable cells.

may have a leukemogenesis capacity in myeloid lineage, because human cell line MV411 was established from acute myeloid leukemia expressing MLL-AF4, several MLL-AF4 mice model developed myeloid leukemia [9], and clinical case sometimes showed lymphoid/myeloid MLL [4]. Therefore, we investigated the mechanism involved in the synergistic effects of MLL-AF4 and Flt3-TKD in 32Dc.

Subsequently, we investigated the antiapoptosis effects of Annexin-V expression. In the MLL-AF4–expressing 32Dc ($32Dc^{MLL\text{-}AF4}$), $32Dc^{Flt3\text{-}TKD}$, and $32Dc^{Flt3+MLL\text{-}AF4}$ cells, apoptosis was induced in the absence of IL-3. However, the $32Dc^{Flt3\text{-}ITD}$ and $32Dc^{Flt3\text{-}TKD+MLL\text{-}AF4}$ cells had acquired a resistance to apoptosis even in the absence of IL-3 (Fig. 3A).

STAT5 is found to be constitutively activated in several samples from patients with leukemia and is strongly activated by Flt3-ITD [21,22]. The serine-threonine kinase Pim-2 is a functionally relevant downstream target of STAT5 [23]. Pim-2 leads to resistance to apoptosis and its expression is negatively regulated by growth factor withdrawal [22,24]. Here, we compared the STAT5 activation and Pim-2 expression potential of 32Dc cells in which each construction was introduced. As shown in Figure 3B, we observed constitutive phosphorylation of STAT5, and a strong induction of Pim-2 in $32Dc^{Flt3\text{-}TKD+MLL\text{-}AF4}$ and $32Dc^{Flt3\text{-}ITD}$ cells, which were starved from IL-3. However, $32Dc^{Flt3\text{-}TKD}$ cells induced a very weak activation of STAT5 and induction of Pim-2 compared to the effects of $32Dc^{Flt3\text{-}TKD+MLL\text{-}AF4}$ and $32Dc^{Flt3\text{-}ITD}$ cells (Fig. 3B).

Differing from previous studies [22], the $32Dc^{Flt3\text{-}TKD}$ cells did not proliferate in the absence of IL-3. This was possibly because Flt3-TKD protein expression in the $32Dc^{Flt3\text{-}TKD}$ cells was low, with low phosphorylation activity, as shown in Figure 1. Thus, Flt3-TKD and MLL-AF4 facilitated independent proliferation of the $32Dc^{Flt3\text{-}TKD+MLL\text{-}AF4}$ cells in the absence of IL-3 via their synergistic leukemogenesis capacity and antiapoptosis effects.

*Flt3-ITD and MLL-AF4 + Flt3-TKD – induced clonogenic growth of 32Dc cells in semisolid media*

To confirm the synergistic antiapoptosis effects of Flt3-TKD and MLL-AF4, we conducted an experiment involving IL-3 removal-related apoptosis induction on semisolid methylcellulose media. As reported in previous studies [22], neither the $32Dc^{Flt3\text{-}TKD}$ nor $32Dc^{MLL\text{-}AF4}$ cells proliferated in the absence of IL-3 in our experiment (Fig. 4A). However, the $32Dc^{Flt3\text{-}ITD}$ and $32Dc^{Flt3\text{-}TKD+MLL\text{-}AF4}$ cells proliferated (Fig. 4A). Furthermore, we compared the number of colonies. The number of colonies formed by the $32Dc^{Flt3\text{-}TKD+MLL\text{-}AF4}$ cells ($16.67 \pm 2.603$) in the absence of IL-3 was lower than that formed by the $32Dc^{Flt3\text{-}ITD}$ cells ($49 \pm 2.082$) ($^*p = 0.002$) (Fig. 4B). There was a difference in the proliferative capacity, as demonstrated in an experiment using liquid media. Thus, the 32Dc cells also showed an independent proliferative capacity on semisolid media in the absence of IL-3 via the synergistic effects of MLL-AF4 and Flt3-TKD.

*Resistance of Flt3-TKD and MLL-AF4 to myeloid differentiation in the presence of G-CSF*

When G-CSF is added to 32Dc cells in the absence of IL-3, these cells differentiate into granulocytes [25]. We investigated the influence of MLL-AF4/Flt3 abnormalities on the differentiation of 32Dc cells (Fig. 5). The rates of blasts and granulocytes 3 days after G-CSF addition were 5.3% ± 2.51% and 81.0% ± 4.00%, respectively, suggesting the differentiation of 32Dc cells. The Flt3–expressing 32Dc ($32Dc^{Flt3}$), $32Dc^{MLL\text{-}AF4}$, and Flt3 + MLL-AF4–expressing 32Dc ($32Dc^{Flt3+MLL\text{-}AF4}$) cells slowly differentiated into granulocytes; 5 days after G-CSF addition, the rate of granulocytes was approximately 60% (Fig. 5). However, there was no differentiation of $32Dc^{Flt3\text{-}TKD+MLL\text{-}AF4}$ nor $32Dc^{Flt3\text{-}ITD}$ cells into granulocytes 9 days after G-CSF addition (Fig. 5). In the $32Dc^{Flt3\text{-}TKD}$ cells, the rates of intermediates and granulocytes were 57.0% ± 10.5% and 22.7% ± 8.62% 5 days after G-CSF addition, respectively, suggesting that differentiation was delayed in the presence of G-CSF (Fig. 5B).

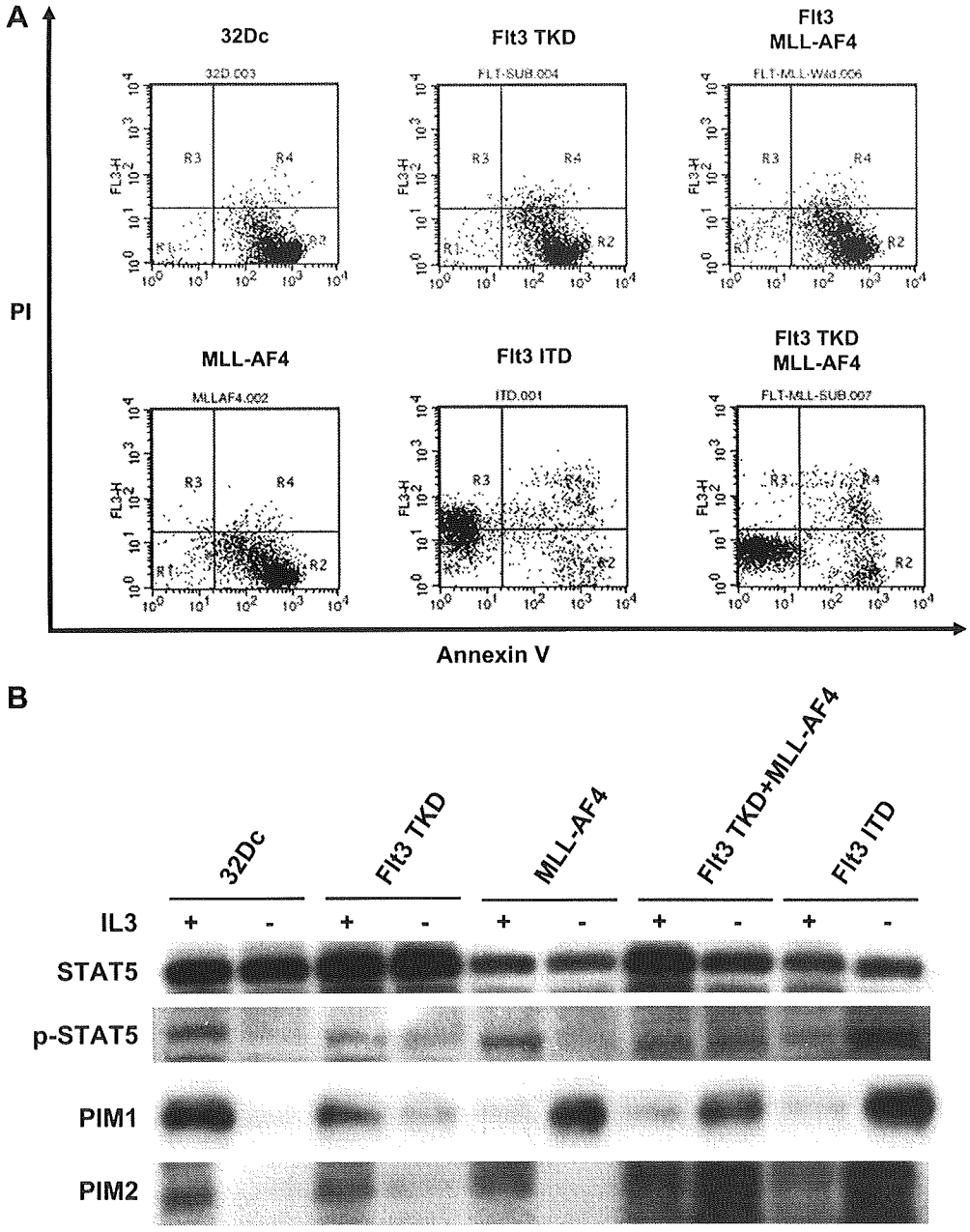


**Figure 3.** Analysis of apoptosis induction in the absence of interleukin-3 (IL-3) in individual gene-transduced 32Dc cells. (**A**) In the absence of IL-3, cell culture was performed. 32Dc cells were stained with allophycocyanin, Annexin-V, and propidium iodide (PI) on day 3, and the other cells on day 7. We analyzed apoptosis induction by flow cytometry. (**B**) Differential signal transducers and activators of transcription 5 (STAT5) and Pim-2 activation in the absence of IL-3. 32Dc cells expressing each genes were starved from IL-3, cell culture was performed for 12 hours, and cell lysates were prepared and subjected to immunoblotting using specific antibodies.

However, 9 days after G-CSF addition, the rate of granulocytes was 77.2% ± 10.9%; most $32Dc^{Flt3\text{-}TKD}$ cells differentiated into granulocytes. Thus, differentiation into granulocytes was inhibited via the synergistic effects of MLL-AF4 and Flt3-TKD. Furthermore, Flt3-TKD inhibited differentiation, although its effects were less marked than those of Flt3-ITD and Flt3-TKD + MLL-AF4.

*Gene expression profiling in the MLL-AF4- and Flt3-TKD + MLL-AF4-transduced cells*

Our experiments regarding the independent proliferative capacity in the absence of IL-3, antiapoptosis actions, and the G-CSF–related induction of differentiation showed that the leukemia proliferation capacity of MLL-AF4 alone was less marked, suggesting the necessity of a second hit contributing to the synergistic effects, as

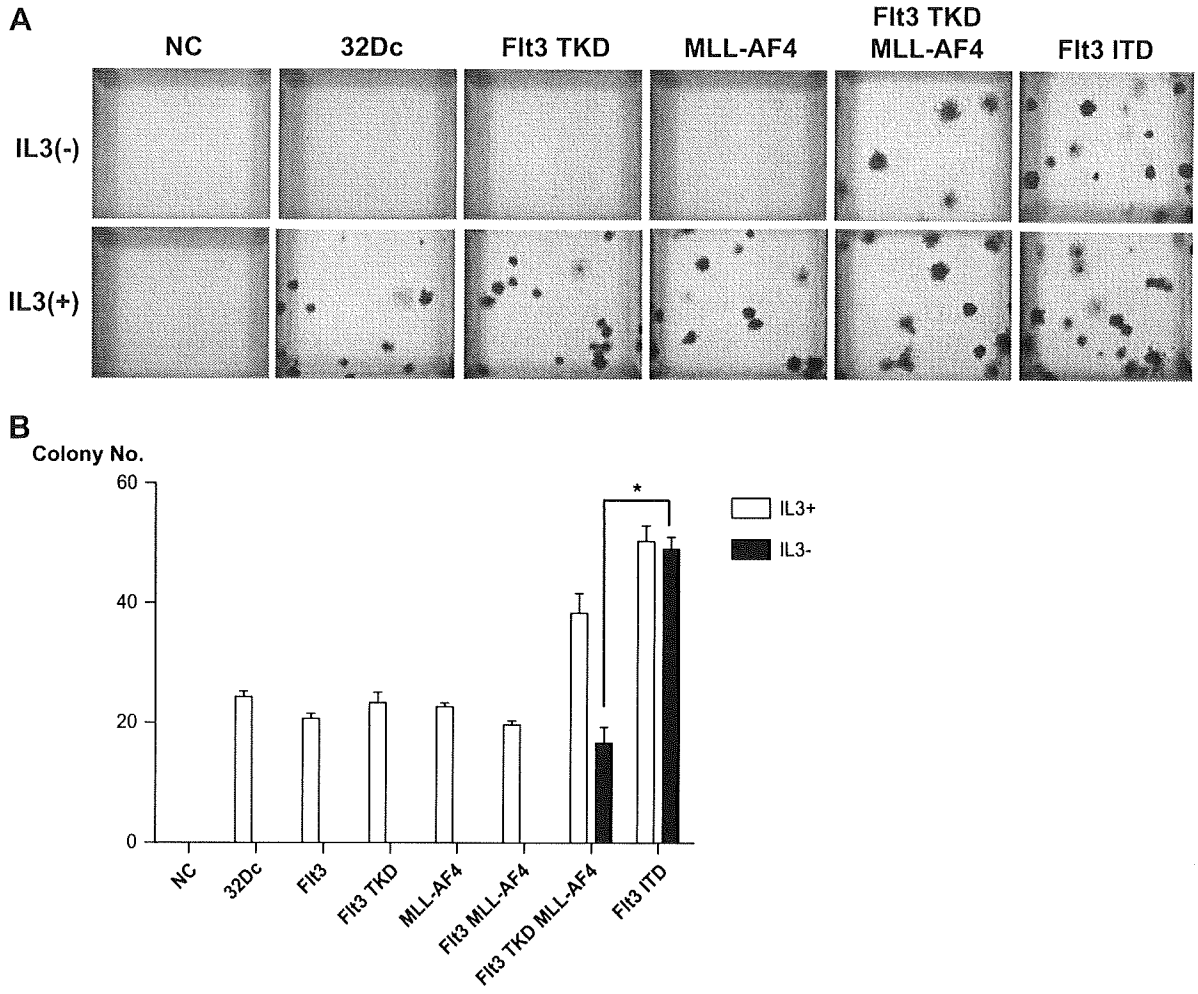


**Figure 4.** Fms-like tyrosine kinase 3 (Flt3) internal tandem duplication (ITD) or Flt3-TKD + MLL-AF4 expression induced colonogenic growth of 32Dc cells in the absence of interleukin-3 (IL-3) semisolid media. (**A**) Colonies were examined using a TE300-DEFS fluorescence inverted phase microscope (Nikon, Tokyo, Japan) with a 4× objective lens. Using a Nikon PDMC II i digital camera, colony assay findings were photographed. The upper and lower rows show the results on day 7 of culture on semisolid methylcellulose media in the absence of IL-3 and in the presence of IL-3, respectively. NC = medium on which no cell was disseminated as a negative control. (**B**) Number of colonies in each cell line on day 7 of culture. $*p = 0.002$.

demonstrated for Flt3-TKD. The activation of Hox genes, such as Hoxa7 and Hoxa9, may be involved in the leukemogenesis of MLL chimeric proteins [2,3]. Therefore, we performed gene expression profiling in the $32Dc^{MLL\text{-}AF4}$ and $32Dc^{Flt3\text{-}TKD+MLL\text{-}AF4}$ cells, and investigated the mechanism involved in the synergistic effects of MLL-AF4 and Flt3-TKD.

Using the Mouse Genome 430 2.0 probe array (Affymetrix), we performed gene expression profiling: 32Dc vs $32Dc^{MLL\text{-}AF4}$, 32Dc vs $32Dc^{Flt3\text{-}TKD+MLL\text{-}AF4}$, and $32Dc^{MLL\text{-}AF4}$ vs $32Dc^{Flt3\text{-}TKD+MLL\text{-}AF4}$. The filing of less reliable data was performed based on Detection Call as a parameter of the reliability of each signal value. Subsequently, expression was compared based on Comparison Call as a parameter of the reliability of gene changes. Initially, in the comparison of 32Dc vs $32Dc^{Flt3\text{-}TKD+MLL\text{-}AF4}$, genes with a twofold or more (log ratio: 1 or more) increase in expression were extracted. Then, in the comparisons of 32Dc vs $32Dc^{MLL\text{-}AF4}$ and $32Dc^{MLL\text{-}AF4}$ vs $32Dc^{Flt3\text{-}TKD+MLL\text{-}AF4}$, genes with an approximate 1.5-fold or greater (log ratio: 0.5 or more) increase in expression were extracted (Table 1). Interestingly, Flt3 abnormalities and/or MLL-AF4 transduction did not indicate enhancement of the expression of Hox genes such as Hoxa7, Hoxa9, and Meis1. Therefore, the expressions of these genes were analyzed by RT-PCR and real-time PCR, but no enhancement was observed (Fig. 6). Among the genes with an increase in expression, we focused on S100A6 (NM_011313), which is involved in the control of cell proliferation.

### *MLL-AF4 and Flt3 abnormality synergistically increased the expression of S100A6*

On real-time PCR, we confirmed S100A6 expression in individual cells. S100A6 expressions in the $32Dc^{Flt3\text{-}TKD}$ and

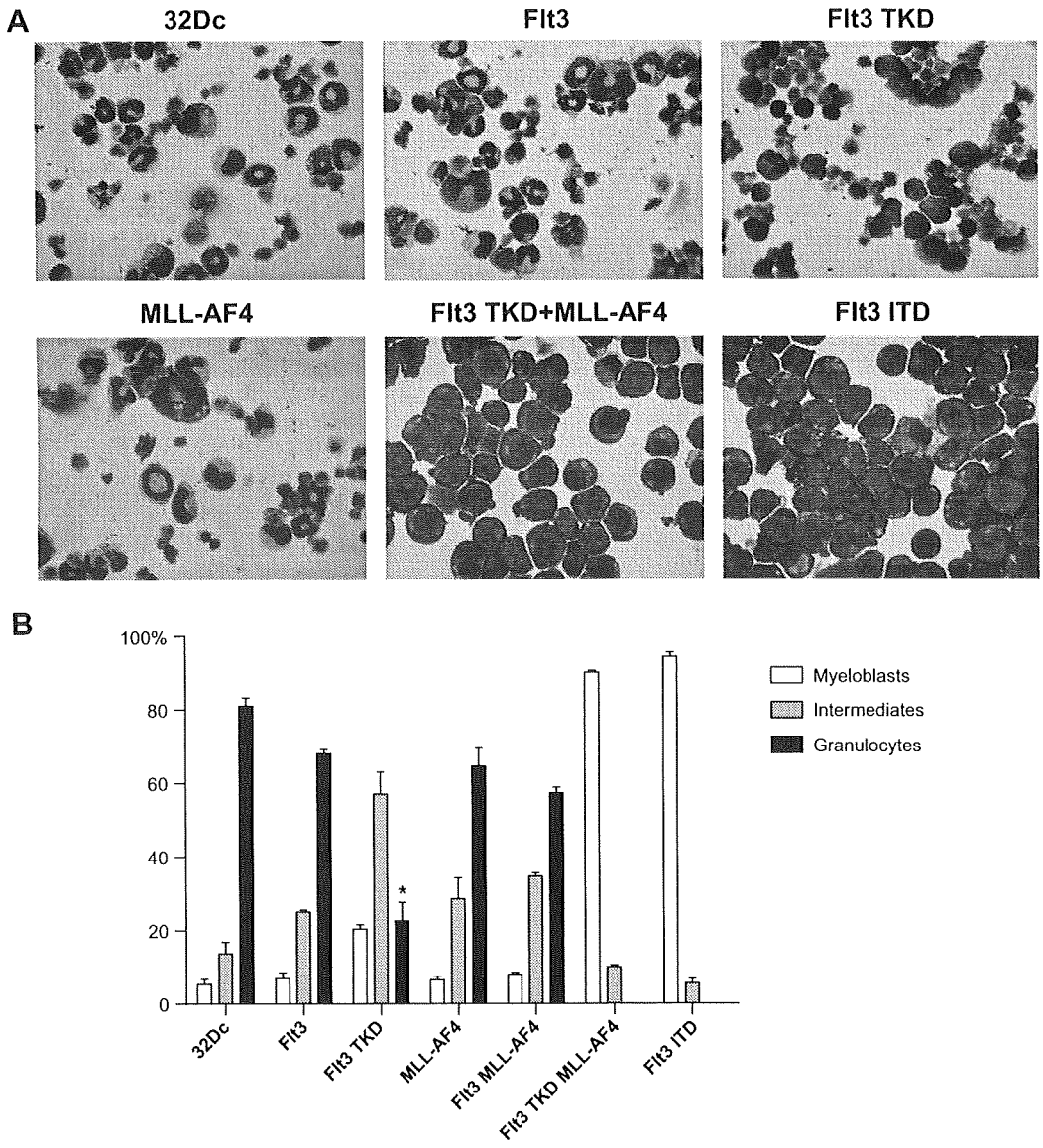


**Figure 5.** Fms-like tyrosine kinase 3 (Flt3) internal tandem duplication (ITD)– and Flt3-TKD + MLL-AF4–related inhibition of the morphologic differentiation of 32Dc cells into granulocytes. After each cell was washed, the medium was exchanged for interleukin-3 (IL-3) –free culture medium containing granulocyte colony-stimulating factor (G-CSF) (10 ng/mL), and observed for 9 days. (**A**) Cytospin samples of 32Dc cells were prepared on day 3, and those of the other cells were prepared on day 5. Microscopy was performed at a magnification ratio of 100. Photographs were prepared. (**B**) Cell differentiation into granulocytes was classified into three steps: blasts, intermediates, and granulocytes. The cell count was measured on day 5. The intermediates included promyelocytes, myelocytes, and metamyelocytes. The $32Dc^{TKD}$ differentiation was delayed in the presence of G-CSF on day 5. (* vs 32Dc: $p = 0.009$, vs $32Dc^{Flt3}$: $p = 0.012$, vs $32Dc^{MLL\text{-}AF4}$: $p = 0.009$, vs $32Dc^{Flt3+MLL\text{-}AF4}$: $p = 0.021$).

$32Dc^{MLL\text{-}AF4}$ cells were two times greater than that in the 32Dc cells ($32Dc^{Flt3\text{-}TKD}$: ×1.96, $p = 0.11$, $32Dc^{MLL\text{-}AF4}$: ×1.82, $p = 0.04$). In the $32Dc^{Flt3\text{-}TKD+MLL\text{-}AF4}$ cells, S100A6 expression increased 13.4-fold, suggesting the synergistic effects of MLL-AF4 and Flt3-TKD (Fig. 7A) (*, **$p < 0.0001$). In addition, among human cell lines, in MV411 cells with both MLL-AF4 and Flt3-ITD abnormalities, S100A6 expression was more than five times greater than those in RS411 cells expressing MLL-AF4 alone and TK cells that we established (RS411 vs MV411: ×5.83, *$p = 0.006$, TK cell vs MV411: ×5.86, **$p = 0.001$) (Fig. 7B). In the $32Dc^{Flt3\text{-}TKD+MLL\text{-}AF4}$, and MV411 cells with high S100A6 expressions on real-time PCR, Western blotting showed protein expression (Fig. 7C).

### *siRNA downregulates synergistic expression of S100A6 and leukemic proliferation*

To confirm that the synergistic enhancement of S100A6 expression had an important role in the leukemogenesis of $32Dc^{Flt3\text{-}TKD+MLL\text{-}AF4}$, we investigated whether anti-S100A6 siRNA-A and -B specifically inhibits S100A6 expression. Real-time PCR and Western blotting analysis

**Table 1.** Genes with the enhancement of their expressions in gene chip analysis.

| Seq ID | Gene Symbol | 32Dc vs $32Dc^{MLL-AF4}$ (log ratio) | 32Dc vs $32Dc^{Flt3TKD\ MLL-AF4}$ (log ratio) | $32Dc^{MLL-AF4}$ vs $32Dc^{Flt3TKD\ MLL-AF4}$ (log ratio) |
|---|---|---|---|---|
| XM_904631 | LOC630963 | 0.7 | 5.6 | 5.2 |
| NM_011347 | Selp | 0.8 | 4.9 | 4.3 |
| NM_026018 | Pdzk1ip1 | 0.9 | 4.3 | 3.4 |
| NM_011578 | Tgfbr3 | 1.1 | 3.9 | 2.9 |
| NM_015734 | Col5a1 | 0.6 | 3.9 | 2.5 |
| NM_008357 | Il15 | 0.7 | 3.5 | 2.6 |
| NM_011578 | Tgfbr3 | 0.9 | 3.4 | 2.7 |
| NM_013516 | Ms4a2 | 1.1 | 3.1 | 1.9 |
| NM_008572 | Mcpt8 | 0.6 | 2.9 | 2.4 |
| NM_145581 | Siglecf | 1.9 | 2.8 | 1 |
| NM_030691 | Igsf6 | 1.9 | 2.7 | 1.4 |
| NM_054041 | Antxr1 | 0.6 | 2.4 | 1.9 |
| NM_013516 | Ms4a2 | 0.6 | 2.1 | 1.7 |
| NM_023605 | Fbxo9 | 0.6 | 2.1 | 1.5 |
| NM_011313 | S100a6 | 1.2 | 2 | 0.8 |
| NM_011346 | Sell | 0.7 | 2 | 1.3 |
| NM_009099 | Trim30 | 1.4 | 1.9 | 0.6 |
| NM_023628 | Anxa9 | 0.7 | 1.9 | 1.4 |
| NM_022881 | Rgs18 | 0.6 | 1.9 | 1.3 |
| NM_007972 | F10 | 0.6 | 1.9 | 1.1 |
| NM_008099 | Gcet2 | 0.5 | 1.8 | 1.1 |
| NM_008771 | P2rx1 | 1 | 1.7 | 0.9 |
| NM_016872 | Vamp5 | 0.5 | 1.7 | 1.2 |
| NM_011609 | Tnfrsf1a | 0.9 | 1.6 | 0.6 |
| XM_905537 | LOC632191 | 0.5 | 1.6 | 1.8 |
| NM_011932 | Dapp1 | 0.8 | 1.5 | 0.8 |
| NM_030684 | Trim34 | 0.7 | 1.5 | 0.8 |
| NM_011488 | Stat5a | 0.5 | 1.4 | 1.1 |
| NM_031198 | Tcfec | 0.7 | 1.3 | 0.5 |
| NM_010739 | Muc13 | 0.6 | 1.3 | 0.7 |
| NM_133948 | Psip1 | 0.6 | 1.3 | 0.7 |
| NM_021389 | Sh3kbp1 | 0.6 | 1.3 | 0.7 |
| NM_001040080 | Ctse | 0.5 | 1.3 | 0.7 |
| NM_009023 | Rapsn | 0.7 | 1.2 | 0.6 |
| NM_010785 | Mdm1 | 0.5 | 1.2 | 0.5 |
| NM_009764 | Brca1 | 0.5 | 1.2 | 0.7 |
| XM_484752 | Zfp236 | 0.5 | 1.2 | 0.6 |
| NM_053272 | Dhcr24 | 0.6 | 1.1 | 0.5 |
| NM_011284 | Rpa2 | 0.6 | 1.1 | 0.5 |
| NM_007791 | Csrp1 | 0.5 | 1.1 | 0.6 |
| NM_172756 | Ankrd41 | 0.5 | 1.1 | 0.6 |

The fold change from log ratios was calculated as $2^{signal\ log\ ratio}$. The purpose of gene expression profiling in this study was screening to extract genes involved in the synergistic effect of Flt3TKD and MLL-AF4. Since cloned cell lines were used as materials, gene expression profiling was performed once. The data of gene expression profiling in this study are in the NCBI's GEO database (GEO accession No.: GSE 14236).

revealed that 24 hours following transfection, S100A6 expression was strongly reduced in $32Dc^{Flt3\text{-}TKD+MLL\text{-}AF4}$ compared with controls transfected with mismatched control SNC1 (Fig. 8A). Then, we assessed whether the downregulation of S100A6 had an effect on $32Dc^{Flt3\text{-}TKD+MLL\text{-}AF4}$ proliferation. As shown in Figure 8B, the anti-S100A6 siRNAs did not affect $32Dc^{Flt3\text{-}TKD+MLL\text{-}AF4}$ proliferation in suspension culture with IL-3. However the anti-S100A6 siRNAs-treated $32Dc^{Flt3\text{-}TKD+MLL\text{-}AF4}$ showed a strong tendency toward reduced cell proliferation in suspension culture without IL-3. Thus, in the presence of Flt3-TKD as a second hit, MLL-AF4 may synergistically promote leukemic proliferation via the enhancement of S100A6 expression.

## Discussion

It has been shown that a second hit is necessary for the mechanism by which MLL-AF4 causes leukemia. Gene expression profiling revealed the enhancement of Flt3

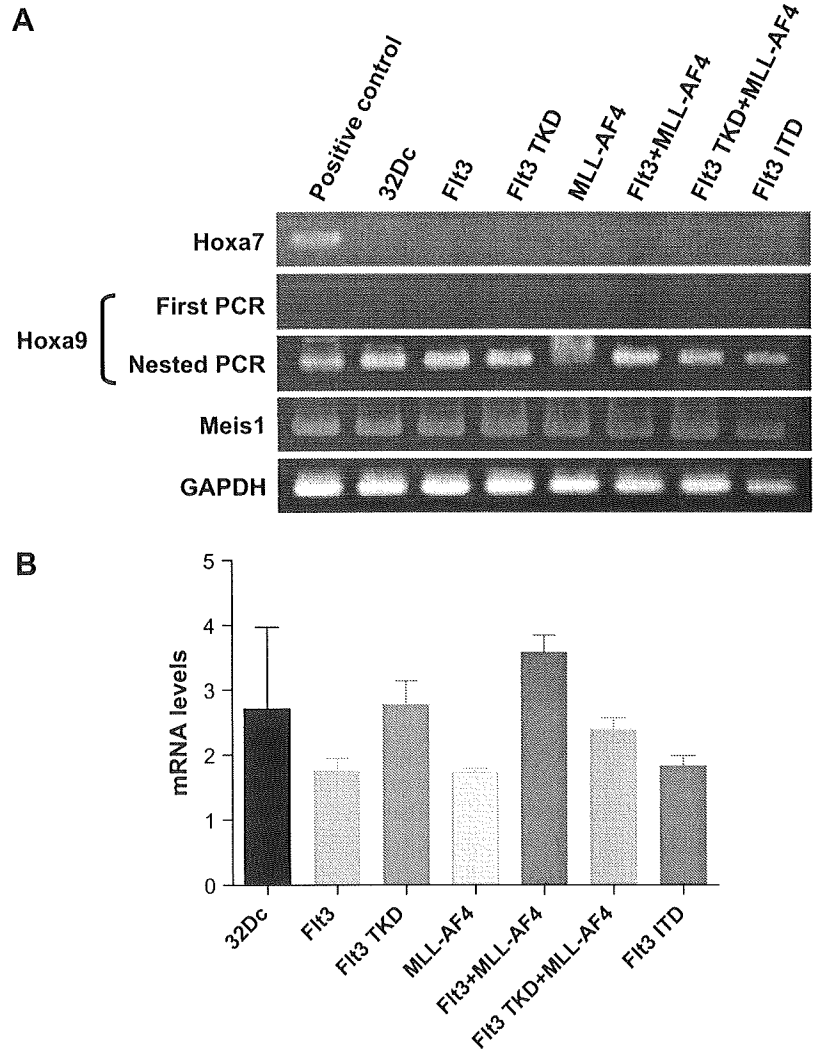


**Figure 6.** Fms-like tyrosine kinase 3 (Flt3) abnormalities and/or MLL-AF4 transduction did not indicate enhancement of the expressions of Hox genes. (**A**) Mouse Hoxa7, Hoxa9, and Meis1 expression in 32Dc cells expressing each gene by reverse transcription polymerase chain reaction (RT-PCR). We used mouse erythroleukemia cells as a positive control. For Hoxa9, because we also obtained no band in the positive control by the first PCR, nested PCR was performed. (**B**) Meis1 expression in 32Dc cells expressing each gene by real-time PCR. No Hoxa7 expression was observed even in 32Dc cells expressing Flt3 abnormality or MLL-AF4, and the level of Hoxa9 expression was negligible. Therefore, real-time PCR for these genes was not performed. Meis1 expression was not also enhanced by Flt3 abnormality or MLL-AF4.

expression in patients with de novo MLL translocation leukemia [12]. In approximately 15% of them, Flt3-TKD abnormalities were observed [13,14]. Therefore, Flt3-TKD may be the first candidate for the second hit. We initially reported that Flt3-TKD, as a second hit, was necessary for MLL-AF4–associated leukemic proliferation in vitro. Furthermore, the two genes synergistically increased the expression of S100A6, and anti-S100A6 siRNA down-regulated leukemic proliferation. This result suggests that the synergistic enhancement of S100A6 expression has an important role in the pathogenesis of MLL-AF4–associated leukemogenesis.

According to previous studies, the leukemogenesis capacity differs between Flt3-TKD and Flt3-ITD [22,26,27]. In vitro analysis showed that the cell-proliferating responsiveness of Flt3-ITD to IL-3 and Flt3 ligands was more marked than that of Flt3-TKD, indicating the less potent inhibitory effects of Flt3 tyrosine kinase inhibitors on cell proliferation [22]. In an in vivo study, Flt3-ITD–expressing mice developed myeloproliferative disease after 1 month, whereas Flt3-TKD–expressing mice developed malignant T-cell lymphoma and acute B-cell lymphatic leukemia after 2 to 4 months [27]. Furthermore, phenotypes depended on the expression of Flt3-ITD; in mice with a low Flt3-ITD expression, the interval until the onset of myeloproliferative disease was longer than that in mice with a high Flt3-ITD expression, and its incidence was lower [27]. These findings suggest that Flt3-TKD is advantageous for the onset of lymphatic malignancy, although its tumor proliferation capacity is less potent than

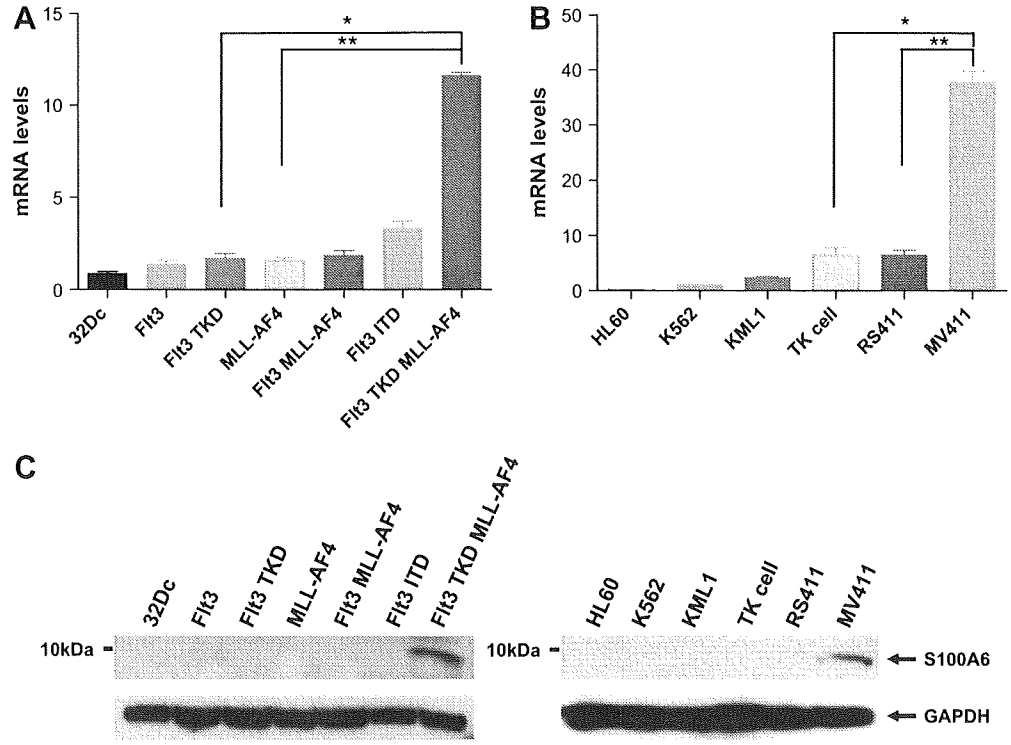


**Figure 7.** Enhancement of S100A6 gene expression via the synergistic effects of Flt3 abnormalities and MLL-AF4. (**A**) Mouse S100A6 expression in 32Dc cells expressing each genes. *$p < 0.0001$; **$p < 0.0001$. (**B**) Human S100A6 expression in human hematopoietic tumor cell lines. *$p = 0.006$, **$p = 0.001$. (**C**) The upper and lower rows show S100A6 (6 kDa) and glyceraldehyde-3-phosphate dehydrogenase (GAPDH) protein expression by Western blotting.

that of Flt3-ITD. In our study, the $32Dc^{Flt3\text{-}TKD}$ cells did not acquire any non – IL-3–dependent proliferative capacity on liquid media, differing from previous studies (Fig. 2) [22]. This was possibly because the leukemic proliferation capacity of Flt3-TKD was less potent than that of Flt3-ITD, and because the transduction efficiency of the TKD-expressing vector was slightly low, reducing its protein expression (Fig. 1).

In our study, 32Dc cells to which MLL-AF4 alone was transduced did not acquire any non – IL-3–dependent proliferative capacity, as demonstrated for the $32Dc^{Flt3\text{-}TKD}$ cells. Joh et al. [28] also transduced MLL-AF9 or MLL-ENL alone to 32Dc cells. However, no non – IL-3–dependent proliferative capacity was achieved [28], as demonstrated in our study. These results suggest that the non – IL-3–dependent proliferation of 32Dc cells cannot be achieved only via the leukemogenesis capacity of MLL-fusion proteins. In MLL-CBP knockin mice, MLL-CBP expression alone did not lead to the onset of hematopoietic malignancies. Administration of N-ethyl-N-nitrosourea–like carcinogenic substances or irradiation in combination with MLL-CBP expression resulted in the onset of myeloproliferative disease [29]. According to several studies in MLL-AF4 expressing mice [9,10], the interval until the onset of hematopoietic malignancies was long, suggesting that the leukemogenesis capacity of MLL-AF4 is not strong; leukemia is not caused via their capacity alone. However, when class II mutations with a weak leukemogenetic capacity, AML1-MTG8 [30] and PML–retinoic acid receptor-α [31], are combined with a class I mutation, Flt3-ITD, they rapidly cause leukemia, as demonstrated for MLL-SEPT6 [18]. In our study, the $32Dc^{Flt3\text{-}TKD+MLL\text{-}AF4}$ cells acquired a non – IL-3-dependent proliferative capacity, and inhibited G-CSF–related differentiation into granulocytes, suggesting the acquisition of the proliferative capacity and the enhancement of the differentiation-inhibiting capacity via the synergistic effects of MLL-AF4 and Flt3-TKD. In the future, both MLL-AF4 and Flt3-TKD–expressing mice should be made and examined.

As the mechanism by which MLL fusion proteins such as MLL-AF4 are involved in leukemogenesis, several studies have indicated that it is important for MLL-AF4 to comprise a complex with menin and directly bind to the promoter of Hox genes, increasing the expressions of Hox genes such as Hoxa7 and Hoxa9 [32–39]. However, the enhancement of Hoxa7/Hoxa9 expressions may not always be necessary for leukemogenesis associated with MLL fusion proteins for the following reasons: first, in an MLL-AF4–expressing cell line, BLIN-3, neither Hoxa7 nor Hoxa9 expressions were detected [40]; second, the transduction of MLL-GAS7 to hematopoietic progenitor cells from Hoxa7/Hoxa9 knockout mice led to leukemogenesis [41]; and third, the condition was modified via mating between MLL-AF9 knockin mice and Hoxa7/Hoxa9 knockout mice, but there were no marked changes, such as complete inhibition of leukemic onset

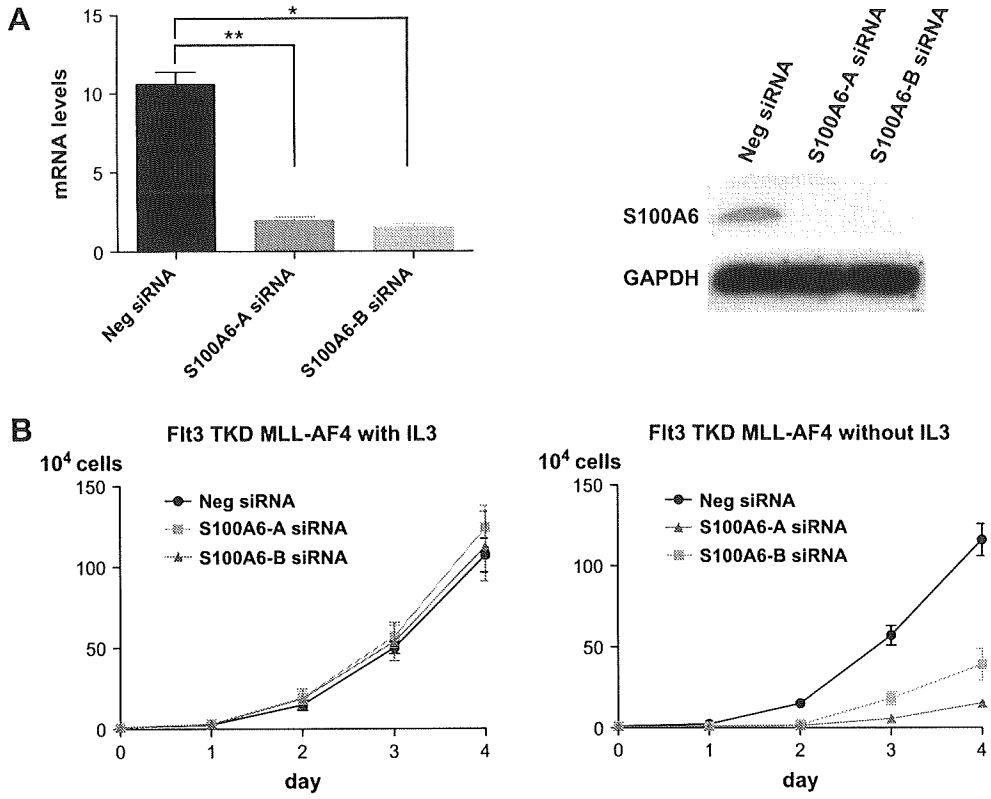


**Figure 8.** Small interfering RNA (siRNA) downregulates synergistic expression of S100A6 and leukemic proliferation. (**A**) Anti-S100A6 siRNA-A and -B mediated the reduction of S100A6 mRNA and protein expression in $32Dc^{Flt3\text{-}TKD+MLL\text{-}AF4}$ without interleukin-3 (IL-3). The left figure show messenger RNA (mRNA) expression by real-time polymerase chain reaction (PCR), and the right figure show protein expression by Western blotting. S100A6 expression levels were measured 24 hours after electroporation, and are shown compared with negative control siRNA (SNC1). $*p = 0.008$; $**p = 0.008$. (**B**) Growth curves of siRNA-treated $32Dc^{Flt3\text{-}TKD+MLL\text{-}AF4}$ with or without IL-3. Downregulation of S100A6 was maintained during a 72-hour period. For 4 days after the start of culture, dead cells were removed using the trypan blue assay, and cell growth curves were drawn based on the number of viable cells.

[42]. The present gene expression analysis did not show the enhancement of Hox gene expression in the $32Dc^{MLL\text{-}AF4}$ or $32Dc^{Flt3\text{-}TKD+MLL\text{-}AF4}$ cells (Fig. 6). Therefore, we focused on S100A6, of which the expression was enhanced in the $32Dc^{Flt3\text{-}TKD+MLL\text{-}AF4}$ cells, as a gene that may contribute to MLL-AF4–associated leukemogenesis, other than Hox genes. S100A6 (calcyclin) is an S100A calcium-binding protein family. Its structure involves the EF-hand motif, which is the site of Ca-binding. S100A6 functions in intracellular Ca homeostasis, signal transmission [43], and regulation of insulin secretion by pancreatic β cells [44]; however, many aspects remain to be clarified. Several studies reported that S100A6 expression was enhanced in patients with various tumors, including acute myelocytic leukemia, colorectal cancer, and pancreatic cancer [45–49]. In particular, the association of S100A6 with disease progression, such as tumor metastasis, is suggested [46,47]. Furthermore, treatment with antisense S100A6 for pulmonary fibroblasts inhibits their proliferation [50]. Results of this study also suggest that S100A6 expression increases via the synergistic effects of MLL-AF4 and Flt3 abnormalities. Moreover, anti-S100A6 siRNA downregulates leukemic proliferation. From the facts described here, we conclude that the synergistic enhancement of S100A6 expression played an important role in MLL-AF4–associated leukemogenesis.

Finally, several limitations of our study merit attention because our results were based on only one cell line in vitro experiment. In most patients with leukemia showing MLL-AF4 expression, Hox gene group expression is increased, which may play an important role in the development of leukemia. However, in 32Dc cells expressing MLL-AF4, Hox gene expression was not enhanced. Therefore, it is questionable that our experiment represents the actual pathology of patients with de novo leukemia showing MLL-AF4 expression. To confirm leukemogenesis of MLL-AF4 in lymphoid lineage and synergistic effect of MLL-AF4 and Flt3-TKD, it is necessary to inspect our results in using primary bone marrow cells or in vivo experiment.

## Acknowledgment

No financial interest/relationships with financial interest relating to the topic of this article have been declared.

## References


1. Rowley JD. The critical role of chromosome translocations in human leukemias. Annu Rev Genet. 1998;32:495–519.
2. Ayton PM, Cleary ML. Molecular mechanisms of leukemogenesis mediated by MLL fusion proteins. Oncogene. 2001;20:5695–5707.
3. Ernst P, Wang J, Korsmeyer SJ. The role of MLL in hematopoiesis and leukemia. Curr Opin Hematol. 2002;9:282–287.
4. Pui CH, Gaynon PS, Boyett JM, et al. Outcome of treatment in childhood acute lymphoblastic leukaemia with rearrangements of the 11q23 chromosomal region. Lancet. 2002;359:1909–1915.
5. Pui CH, Evans WE. Treatment of acute lymphoblastic leukemia. N Engl J Med. 2006;354:166–178.
6. Kersey JH, Wang D, Oberto M. Resistance of t(4; 11) (MLL-AF4 fusion gene) leukemias to stress-induced cell death: possible mechanism for extensive extramedullary accumulation of cells and poor prognosis. Leukemia. 1998;12:1561–1564.
7. Dörrie J, Schuh W, Keil A, et al. Regulation of CD95 expression and CD95-mediated cell death by interferon-gamma in acute lymphoblastic leukemia with chromosomal translocation t(4;11). Leukemia. 1999;13: 1539–1547.
8. Thomas M, Gessner A, Vornlocher HP, et al. Targeting MLL-AF4 with short interfering RNAs inhibits clonogenicity and engraftment of t(4; 11)-positive human leukemic cells. Blood. 2005;106:3559–3566.
9. Chen W, Li Q, Hudson WA, et al. A murine Mll-AF4 knock-in model results in lymphoid and myeloid deregulation and hematologic malignancy. Blood. 2006;108:669–677.
10. Metzler M, Forster A, Pannell R, et al. A conditional model of MLL-AF4 B-cell tumourigenesis using invertor technology. Oncogene. 2006;25:3093–3103.
11. Gilliland DG, Griffin JD. The roles of FLT3 in hematopoiesis and leukemia. Blood. 2002;100:1532–1542.
12. Armstrong SA, Staunton JE, Silverman LB, et al. MLL translocations specify a distinct gene expression profile that distinguishes a unique leukemia. Nat Genet. 2002;30:41–47.
13. Armstron SA, Kung AL, Mabon ME, et al. Inhibition of FLT3 in MLL. Validation of a therapeutic target identified by gene expression based classification. Cancer Cell. 2003;3:173–183.
14. Taketani T, Taki T, Sugita K, et al. FLT3 mutations in the activation loop of tyrosine kinase domain are frequently found in infant ALL with MLL rearrangements and pediatric ALL with hyperdiploidy. Blood. 2004;103:1085–1088.
15. Brown P, Levis M, Shurtleff S, Campana D, Downing J, Small D. FLT3 inhibition selectively kills childhood acute lymphoblastic leukemia cells with high levels of FLT3 expression. Blood. 2005; 105:812–820.
16. Stam RW, den Boer ML, Schneider P, et al. Targeting FLT3 in primary MLL-gene-rearranged infant acute lymphoblastic leukemia. Blood. 2005;106:2484–2490.
17. Brown P, Levis M, McIntyre E, et al. Combinations of the FLT3 inhibitor CEP-701 and chemotherapy synergistically kill infant and childhood MLL-rearranged ALL cells in a sequence-dependent manner. Leukemia. 2006;20:1368–1376.
18. Ono R, Nakajima H, Ozaki K, et al. Dimerization of MLL fusion proteins and FLT3 activation synergize to induce multiple-lineage leukemogenesis. J Clin Invest. 2005;115:919–929.
19. Hanawa H, Persons DA, Nienhuis AW. Mobilization and mechanism of transcription of integrated self-inactivating lentiviral vectors. J Virol. 2005;79:8410–8421.
20. Inokuchi K, Miyake K, Takahashi H, et al. DCC protein expression in hematopoietic cell populations and its relation to leukemogenesis. J Clin Invest. 1996;97:852–857.
21. Mizuki M, Fenski R, Halfter H, et al. Flt3 mutations from patients with acute myeloid leukemia induce transformation of 32D cells mediated by the Ras and STAT5 pathways. Blood. 2000;96:3907–3914.
22. Choudhary C, Schwable J, Brandts C, et al. AML-associated Flt3 kinase domain mutations show signal transduction differences compared with Flt3 ITD mutations. Blood. 2005;106:265–273.
23. Mizuki M, Schwable J, Steur C, et al. Suppression of myeloid transcription factors and induction of STAT response genes by AML-specific Flt3 mutations. Blood. 2003;101:3164–3173.
24. Fox CJ, Hammerman PS, Cinalli RM, et al. The serine/threonine kinase Pim-2 is a transcriptionally regulated apoptotic inhibitor. Genes Dev. 2003;17:1841–1854.
25. Zheng R, Friedman AD, Small D. Targeted inhibition of FLT3 overcomes the block to myeloid differentiation in 32Dcl3 cells caused by expression of FLT3/ITD mutations. Blood. 2002;100: 4154–4161.
26. Grundler R, Thiede C, Miething C, et al. Sensitivity toward tyrosine kinase inhibitors varies between different activating mutations of the FLT3 receptor. Blood. 2003;102:646–651.
27. Grundler R, Miething C, Thiede C, et al. FLT3-ITD and tyrosine kinase domain mutants induce 2 distinct phenotypes in a murine bone marrow transplantation model. Blood. 2005;105: 4792–4799.
28. Joh T, Kagami Y, Yamamoto K, et al. Identification of MLL and chimeric MLL gene products involved in 11q23 translocation and possible mechanisms of leukemogenesis by MLL truncation. Oncogene. 1996;13:1945–1953.
29. Wang J, Iwasaki H, Krivtsov A, et al. Conditional MLL-CBP targets GMP and models therapy-related myeloproliferative disease. EMBO J. 2005;24:368–381.
30. Schessl C, Rawat VP, Cusan M, et al. The AML1-ETO fusion gene and the FLT3 length mutation collaborate in inducing acute leukemia in mice. J Clin Invest. 2005;115:2159–2168.
31. Kelly LM, Kutok JL, Williams IR, et al. PML/RARalpha and FLT3-ITD induce an APL-like disease in a mouse model. Proc Natl Acad Sci U S A. 2002;99:8283–8288.
32. Milne TA, Briggs SD, Brock HW, et al. MLL targets SET domain methyltransferase activity to Hox gene promoters. Mol Cell. 2002; 10:1107–1117.
33. Yeoh EJ, Ross ME, Shurtleff SA, et al. Classification, subtype discovery, and prediction of outcome in pediatric acute lymphoblastic leukemia by gene expression profiling. Cancer Cell. 2002;1: 133–143.
34. Ayton PM, Cleary ML. Transformation of myeloid progenitors by MLL oncoproteins is dependent on Hoxa7 and Hoxa9. Genes Dev. 2003;17:2298–2307.
35. Ferrando AA, Armstrong SA, Neuberg DS, et al. Gene expression signatures in MLL-rearranged T-lineage and B-precursor acute leukemias: dominance of HOX dysregulation. Blood. 2003;102: 262–268.
36. Rozovskaia T, Ravid-Amir O, Tillib S, et al. Expression profiles of acute lymphoblastic and myeloblastic leukemias with ALL-1 rearrangements. Proc Natl Acad Sci U S A. 2003;100:7853–7858.
37. Yokoyama A, Wang Z, Wysocka J, et al. Leukemia proto-oncoprotein MLL forms a SET1-like histone methyltransferase complex with menin to regulate Hox gene expression. Mol Cell Biol. 2004;24: 5639–5649.
38. Zeisig BB, Milne T, Garcia-Cuellar MP, et al. Hoxa9 and Meis1 are key targets for MLL-ENL-mediated cellular immortalization. Mol Cell Biol. 2004;24:617–628.
39. Yokoyama A, Somervaille TC, Smith KS, et al. The menin tumor suppressor protein is an essential oncogenic cofactor for MLL-associated leukemogenesis. Cell. 2005;123:207–218.
40. Bertrand FE, Spengeman JD, Shah N, LeBien TW. B-cell development in the presence of the MLL/AF4 oncoprotein proceeds in the absence of HOX A7 and HOX A9 expression. Leukemia. 2003;17: 2454–2459.

41. So CW, Karsunky H, Wong P, et al. Leukemic transformation of hematopoietic progenitors by MLL-GAS7 in the absence of Hoxa7 or Hoxa9. Blood. 2004;103:3192–3199.
42. Kumar AR, Hudson WA, Chen W, et al. Hoxa9 influences the phenotype but not the incidence of Mll-AF9 fusion gene leukemia. Blood. 2004;103:1823–1828.
43. Courtois-Coutry N, Le Moellic C, Boulkroun S, et al. Calcyclin is an early vasopressin-induced gene in the renal collecting duct. Role in the long term regulation of ion transport. J Biol Chem. 2002;277: 25728–25734.
44. Okazaki K, Niki I, Iino S, et al. A role of calcyclin, a Ca(2+)-binding protein, on the Ca(2+)-dependent insulin release from the pancreatic beta cell. J Biol Chem. 1994;269:6149–6152.
45. Calabretta B, Kaczmarek L, Mars W, et al. Cell-cycle-specific genes differentially expressed in human leukemias. Proc Natl Acad Sci U S A. 1985;82:4463–4467.
46. Komatsu K, Kobune-Fujiwara Y, Andoh A, et al. Increased expression of S100A6 at the invading fronts of the primary lesion and liver metastasis in patients with colorectal adenocarcinoma. Br J Cancer. 2000;83:769–774.
47. Stulik J, Osterreicher J, Koupilova K, et al. Differential expression of the Ca2+ binding S100A6 protein in normal, preneoplastic and neoplastic colon mucosa. Eur J Cancer. 2000;36:1050–1059.
48. Emberley ED, Murphy LC, Watson PH. S100 proteins and their influence on pro-survival pathways in cancer. Biochem Cell Biol. 2004;82: 508–515.
49. Vimalachandran D, Greenhalf W, Thompson C, et al. High nuclear S100A6 (Calcyclin) is significantly associated with poor survival in pancreatic cancer patients. Cancer Res. 2005;65:3218–3225.
50. Breen EC, Tang K. Calcyclin (S100A6) regulates pulmonary fibroblast proliferation, morphology, and cytoskeletal organization in vitro. J Cell Biochem. 2003;88:848–854.

Neurochemistry International 54 (2009) 513–518

Contents lists available at ScienceDirect

Neurochemistry International

journal homepage: www.elsevier.com/locate/neuint

# Therapeutic effect of edaravone on inner ear barotrauma in the guinea pig

Hitoshi Maekawa [a], Takeshi Matsunobu [a,*], Hitoshi Tsuda [b], Kaoru Onozato [b], Yukihiro Masuda [a], Tetsuya Tanabe [a], Akihiro Shiotani [a]

[a] Department of Otolaryngology, National Defense Medical College, Saitama, Japan
[b] Department of Morbid Pathology, National Defense Medical College, Saitama, Japan

ARTICLE INFO

*Article history:*
Received 8 September 2008
Received in revised form 20 January 2009
Accepted 12 February 2009
Available online 24 February 2009

*Keywords:*
ROS
Free radical
Edaravone
Inner ear
Hearing loss

ABSTRACT

Inner ear barotrauma (IEB) that is caused by acute pressure changes can often lead to permanent severe sensorineural hearing loss (SNHL). However, the mechanism that causes IEB is still unknown. In the current study, we assessed the involvement of reactive oxygen species (ROS) in IEB and the therapeutic effect of 3-methyl 1-phenyl-2-pyrazolin-5-one (edaravone), which is a free radical scavenger. To create the IEB model, guinea pigs were subjected to quick pressure changes that resulted in acute SNHL. The animals were then divided into two groups, an edaravone-treated IEB group and a non-treated IEB group that only received normal saline. Immunohistochemical analyses for 8-hydroxy-2-deoxyguanosine (8-OHdG) and 4-hydroxy-2-nonenal (4-HNE) were performed to examine the amount of oxidative DNA damage and lipid peroxidation that occurred in guinea pig cochlea. To assess the curative efficacy of edaravone, auditory brainstem response (ABR) testing was performed to evaluate auditory function. Strong immunoreactivities against 8-OHdG and 4-HNE were observed in the inner ear tissues of the non-treated IEB group. Lesser amounts of immunoreactivity were observed in the same region of the edaravone-treated IEB group as compared to the non-treated IEB group. Furthermore, ABR measurement revealed that there was a faster improvement in the threshold shift for the edaravone-treated IEB group as compared to that of the non-treated IEB group. At the final 7-week time point, the threshold shift for the edaravone-treated IEB group was significantly smaller as compared to the non-treated IEB group. These results strongly suggest that ROS is produced in the cochlea in response to acute pressure changes and that ROS plays an important role in the pathophysiology of IEB. Furthermore, edaravone treatment had a therapeutic effect on IEB-induced acute SNHL and thus, edaravone might possibly be able to be used as a therapeutic treatment for IEB.



## 1. Introduction

Acute pressure changes, such as those that occur during scuba diving, when flying on an airplane, or when blowing ones nose, can cause inner ear barotrauma (IEB). When there is damage to the middle and inner ear, this can lead to sensorineural hearing loss (SNHL). With the increased popularity of scuba diving, many diving enthusiasts now have a higher risk of developing IEB. Today, approximately 1 million people in Japan have taken instructional classes and gone on scuba diving trips. The number of people who repeatedly dive is estimated to be from 300,000 to 500,000 (Nakayama et al., 2003). And as might be expected, ear disease or injury is the most common medical problem seen in scuba divers (Goplen et al., 2007). In addition, acute diving accidents that affect the inner ear are of particular importance because they can lead to permanent damage within the cochleovestibular system (Parell and Becker, 1985). While the increases in the number of cases of IEB that are now being seen indicate that particular attention needs to be paid to this problem, at the present time, the mechanism of IEB has yet to be elucidated.

Recently, compelling studies have shown that there are relationships between reactive oxygen species (ROS) and various types of acute SNHL, such as noise-induced hearing loss (Yamasoba et al., 1998), aminoglycoside ototoxicity (Schacht, 1998), and cisplatin ototoxicity (Ryback et al., 1999). As IEB is one of the causes of acute SNHL, we hypothesized that ROS formation might also be associated with the IEB that occurs within the cochlea. Therefore, we investigated the relationship between ROS and IEB by using the production of 8-hydroxy-2-deoxyguanosine (8-OHdG) to detect oxidative DNA damage and 4-hydroxy-2-nonenal (4-HNE) to detect lipid peroxidation in the organ of Corti, stria vascularis, and spiral ganglion cells.

When treating inner ear disorders that are related to ROS-induced inner ear damage, free radical scavengers have been

* Corresponding author.
*E-mail address:* takeshim@ndmc.ac.jp (T. Matsunobu).

0197-0186/$ – see front matter © 2009 Elsevier Ltd. All rights reserved.
doi:10.1016/j.neuint.2009.02.011

shown to have protective effects against both aminoglycoside-induced ototoxicity (Garetz et al., 1994) and cisplatin-induced ototoxicity (Fetoni et al., 2004). Edaravone is a potent free radical scavenger that exerts significant antioxidant effects on both hydroxyl radicals and iron-dependent lipid peroxidation and thus, can exert anti-ischemic activities (Watanabe et al., 1994). Several studies have shown the effects of edaravone on the inner ear (Tanaka et al., 2005; Maetani et al., 2003).

In the present study, we hypothesized that edaravone might be an effective therapeutic IEB treatment. Therefore, we examined the pathophysiology of IEB and the possible therapeutic application of the free radical scavenger, edaravone, in IEB cases.

## 2. Materials and methods

### 2.1. Animals

This study used healthy female guinea pigs with a normal Preyer's reflex that weighed between 300 and 350 g (Japan SLC, Inc., Shizuoka, Japan). The animals had free access to water and were fed a regular diet. The experiments were carried out under the guidelines for animal experiments of the National Defense Medical College and met the law and notification requirements of the government of Japan.

### 2.2. Pressure loading

Under deep anesthesia that used intraperitoneal injection of ketamine (55 mg/kg) and medetomidine (1.0 mg/kg), earplugs were inserted into the external auditory canal of the animals in order to restrict the movement of the tympanic membrane and to facilitate IEB. Animals were then put into a chamber (Haniuda P-5100, Haniuda Steel, Tokyo, Japan) in which the atmospheric pressure could be increased or decreased (Fig. 1A). When the inflow bulb was opened, compressed air flowed into the chamber and produced pressure. When the outflow bulb was opened, the air in the chamber was discharged with a subsequent decrease in the pressure. In this study, the pressure was increased from 1 atmosphere pressure absolute (ATA) to 2 ATA over a 3-s time period. We used a pressure of 2 ATA in this study, as it is the equivalent of a depth of 10 m, which is the average depth under the water that most scuba divers will attain during a dive. Subsequently we decreased the pressure from 2 to 1 ATA over a 2-s time period (Fig. 1B). After this pressure loading, the earplugs were then immediately removed. In the present study, this system induced IEBs with threshold shifts of 50 dB on average.

### 2.3. Immunohistochemistry of the organ of Corti

Four guinea pigs were exposed to pressure loading sufficient to induce a threshold shift. Immediately after the pressure loading, two animals received an intraperitoneal injection of edaravone (9.0 mg/kg) (Mitsubishi Tanabe Pharma Corporation, Tokyo, Japan) (edaravone-treated IEB group), while the other two animals were injected with normal saline (non-treated IEB group). All animals were sacrificed under deep anesthesia 1 h after the pressure loading. A normal group was also examined and consisted of two animals that were neither exposed to pressure nor to edaravone treatment. All six animals were decapitated, with the temporal bones quickly removed and the bullae opened, followed by transfer to 4% paraformaldehyde in 0.1 M phosphate-buffered saline (PBS, pH 7.4). The bone near the apex, the round window, and the oval window were opened, followed by a gentle local perfusion with 2 × 1 ml of 4% paraformaldehyde. The tissues were kept in the fixative overnight. The cochleae were dissected by removing the lateral wall bones, lateral wall tissues, and the tectorial membranes. After washing with PBS, the remaining parts of the cochlea were incubated in 0.3% Triton X-100 in PBS for 15 min, washed three times, and then, in order to block any non-specific reactions, incubated in blocking solution that consisted of 2% normal swine serum (Dako, Glostrup, Denmark). To detect oxidative DNA damage, immunolabeling was carried out overnight at 4 °C with the mouse monoclonal antibody for 8-OHdG (1:10; Nikken Seil Corporation, Shizuoka, Japan). Sections were washed three times in PBS, and incubated with a secondary antibody (Histofine Simple Stain AP; Nichirei Bioscience, Tokyo, Japan; universal immuno-alkaline-phosphatase polymer) for 30 min at room temperature and then stained using the alkaline phosphatase substrate kits (Vector Black; Vector Laboratories, Burlingame, CA, USA). Finally, whole mount preparations of the basal turn, which is mostly damaged in IEB, of the organ of Corti were prepared, with the immunolabeling visualized under brightfield illumination using an Olympus microscope with a 200× objective. The immunoreactivity of 8-OHdG in the organ of Corti was evaluated and compared among the normal, edaravone-treated, and non-treated IEB groups.

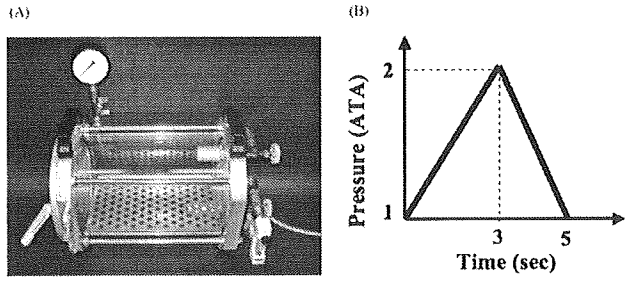


**Fig. 1.** (A) The animal chamber. The chamber was used to increase and decrease the atmospheric pressure. (B) Pressure loading. The pressure was increased from 1 atmosphere pressure absolute (ATA) to 2 ATA over a 3-s time period, and then decreased from 2 to 1 ATA over a 2-s time period.

### 2.4. Immunohistochemistry of the stria vascularis and spiral ganglion cells

Animals were divided into three groups as mentioned above with the edaravone-treated IEB group receiving edaravone (9.0 mg/kg) once a day for 5 days after the pressure loading. Animals were sacrificed under deep anesthesia at 1 week after the pressure loading. The temporal bones were fixed, as has been mentioned above. After decalcification with 0.1 M ethylenediaminetetraacetic acid (EDTA) in PBS for 14 days at 4 °C, 4-μm paraffin sections were prepared. Sections were deparaffinized and then washed three times with PBS. Antigens in the sections were placed in 10 mM citric acid buffer (pH 6.0) after retrieval using a microwave set at 97 °C for 10 min. After washing with PBS three times, the sections were incubated in 2% normal swine serum in order to block any non-specific reactions. In order to assess lipid peroxidation, immunolabeling was carried out overnight at 4 °C with the mouse monoclonal antibody for 8-OHdG (1:10) and with the mouse monoclonal antibody for 4-HNE (1:10; Nikken Seil Corporation). Subsequently, sections were treated with a secondary antibody (Histofine Simple Stain AP) followed by staining with the alkaline phosphatase substrate kits (Vector Black). The immunoreactivities of 8-OHdG and 4-HNE in the stria vascularis and spiral ganglion cells were evaluated and compared among the normal, edaravone-treated, and non-treated IEB groups.

### 2.5. Treatment with edaravone

After the pressure loading, the 30 ears (29 guinea pigs) that showed threshold shifts of more than 30 dB were randomly divided into two groups of 15 ears. The edaravone-treated IEB group received an intraperitoneal injection of edaravone (9.0 mg/kg) once a day for 5 days after the pressure loading, while the non-treated IEB group received normal saline. The remaining 28 ears showed threshold shifts of 30 dB or less were excluded to avoid error of measurement.

### 2.6. Auditory brainstem responses

Auditory brainstem responses (ABR) were measured using a signal recorder (Synax 1200, NEC, Tokyo, Japan), 1 week before the pressure loading, just after the pressure loading, and then at 2, 3, 5, and 7 weeks after the pressure loading. All steps were performed under deep anesthesia that used intraperitoneal injection of ketamine (55 mg/kg) and medetomidine (1.0 mg/kg). A differential active needle electrode was placed at each auricle of the ear while a reference electrode was placed at the vertex. A click at 4 kHz was used for the auditory stimulus followed by the recording of 100 sweeps. As determined by peak I of the waveform, the ABR threshold was recorded from 90 to 20 dB using 10-dB steps. Guinea pigs exhibiting normal ABR thresholds (i.e., less than 40 dB) were enrolled into the experiments. After the pressure loading, if peak I of the waveform was not found, even when using a maximum amplitude (90 dB), the threshold was deemed to be unresponsive and thus considered to be 100 dB.

All data values for the ABR threshold shift in the text and in the figures are the mean standard error (SE). The Repeated Measures ANOVA was used to statistically examine the time course change for the recovery of the ABR threshold shift between the non-treated IEB group and the edaravone-treated IEB group. The ameliorations of the ABR threshold shift at each time point (2, 3, 5, and 7 weeks after the pressure loading) were compared using the Mann–Whitney *U*-test.

## 3. Results

### 3.1. Cochlear histopathology of IEB

The mid-modiolar section of the cochlea 3 h after the pressure loading is shown in Fig. 2. Conglomeration of red blood cells was observed in the scala tympani, scala media, and scala vestibuli, suggesting that it is a cochlear blood flow disturbance or ischemia that leads to the hemorrhage that is observed in IEB. Although old clot of blood was also observed in the inner ear 18 weeks after the pressure loading, new hemorrhage was not observed. Amount of the clot was less than that observed in the animals sacrificed 3 h after the pressure loading. This indicated that hemorrhage has been absorbed

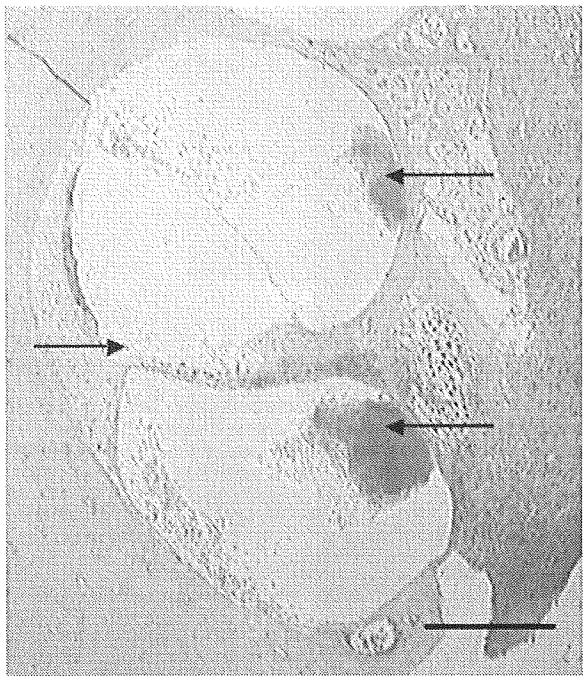

**Fig. 2.** Mid-modiolar section of the cochlea 3 h after the pressure loading. Hemorrhage (arrows) into the scala tymapani, scala media, and scala vestibuli were observed (HE stain). Scale bar = 200 μm.

slightly over time. Obvious hemorrhage was not observed in the mucosa of the middle ear and skin of the external ear.

### 3.2. Immunohistochemistry

In the outer hair cells (OHCs), strong immunoreactivity for 8-OHdG in the nuclei of the OHCs was observed 1 h after the pressure loading in the non-treated IEB group (Fig. 3B). In contrast, there was less immunoreactivity observed in the edaravone-treated IEB group (Fig. 3C) as compared to the non-treated IEB group. Weak immunoreactivity for 8-OHdG was observed in the nuclei of the OHCs of the normal group (Fig. 3A).

In the spiral ganglion cells, strong immunoreactivities for 8-OHdG and 4-HNE were observed in the non-treated IEB group (Fig. 4B and E). Lesser amounts of immunoreactivity were observed in the edaravone-treated IEB group (Fig. 4C and F) as compared to the non-treated IEB group, while weak immunoreactivities were observed in the normal group (Fig. 4A and D).

In the stria vascularis, strong immunoreactivities for 8-OHdG were observed in the nuclei of the marginal cells, intermediate cells, and basal cells of the non-treated IEB group (Fig. 5B), and there were strong immunoreactivities for 4-HNE observed in the cytoplasm of all cell types for the non-treated IEB group (Fig. 5E). Lesser amounts of immunoreactivity for 8-OHdG and 4-HNE were observed in the edaravone-treated IEB group (Fig. 5C and F) as compared to that observed in the non-treated IEB group, while weak immunoreactivities were observed in the normal group (Fig. 5A and D).

### 3.3. ABR

The time course change for the threshold shift after the pressure loading is shown in Fig. 6A. Immediately after the pressure loading, the threshold shift of the edaravone-treated IEB group was 51 ± 4 dB, while that of the non-treated IEB group was 50 ± 4 dB. There was a significantly faster improvement of the threshold shift for the edaravone-treated IEB group as compared to that seen for the non-treated IEB group (Repeated Measures ANOVA, $P = 0.0016$). When the final auditory function was measured at 7 weeks after the pressure loading, the threshold shift of the edaravone-treated IEB group was 18 ± 6 dB with 33-dB ameliorations. The threshold shift for the non-treated IEB group was 30 ± 6 dB with only 20-dB ameliorations. These results were marginally significantly different ($P = 0.0564$, Mann–Whitney $U$-test).

In the clinical cases of sudden deafness, most of the severely damaged ears are not cured and it is difficult to evaluate the pharmaceutical effects against severely damaged ears. Therefore we excluded all animals with severe threshold shifts (scale out and ≥60 dB) and evaluated the therapeutic effect of edaravone on animals whose threshold shifts were less than 50 dB. The time course change for the threshold shift after the pressure loading is shown in Fig. 6B. The threshold shift of the edaravone-treated IEB group exhibited a significantly faster improvement as compared to that of the non-treated IEB group (Repeated Measures ANOVA, $P = 0.0245$). Significant improvement of the threshold shift was observed in the edaravone-treated IEB group at 2 and 7 weeks (Mann–Whitney $U$-test, $P = 0.0118$, $P = 0.0469$).

## 4. Discussion

Barotrauma arises due to atmospheric pressure changes in organs that form a cavity such as the ear, paranasal sinus, and the lung. The frequently occurring aural barotrauma has been classified into three groups: external barotrauma, middle ear barotrauma, and IEB. IEB is the most important of the barotraumas because the hearing loss associated with the IEB can become a permanent and disabling injury of the cochleovestibular system. Although the precise mechanism of IEB has yet to be determined, several hypotheses have been proposed, such as the rupture of Reissner's membrane (Simmons, 1978), round or oval window fistula (Goodhill, 1971), or circulatory disturbances within the

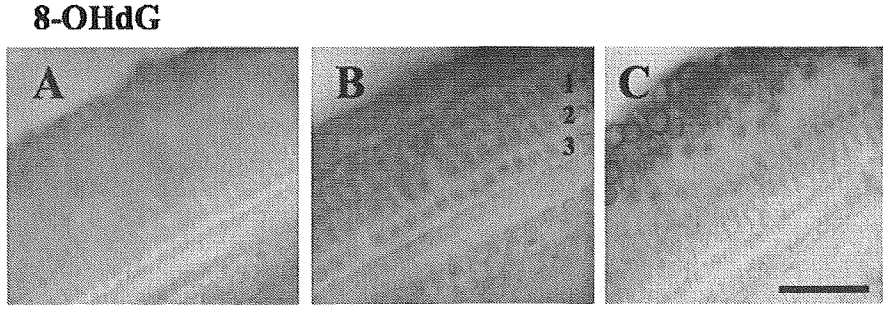


**Fig. 3.** Immunoreactivities of 8-hydroxy-2-deoxyguanosine (8-OHdG) in the organ of Corti. Animals for immunohistochemistry of the organ of Corti were sacrificed 1 h after the pressure loading and the slices were prepared. Three rows of the outer hair cells (OHCs) are indicated by the numbers 1, 2, and 3. Scale bar = 50 μm. (A) Weak immunoreactivity was observed in the OHCs region in the normal group. (B) Strong immunoreactivity was observed in nuclei of the OHCs in the non-treated IEB group. (C) Lesser amounts of immunoreactivity were observed in the same region of the edaravone-treated IEB group as compared to that observed in the non-treated IEB group.

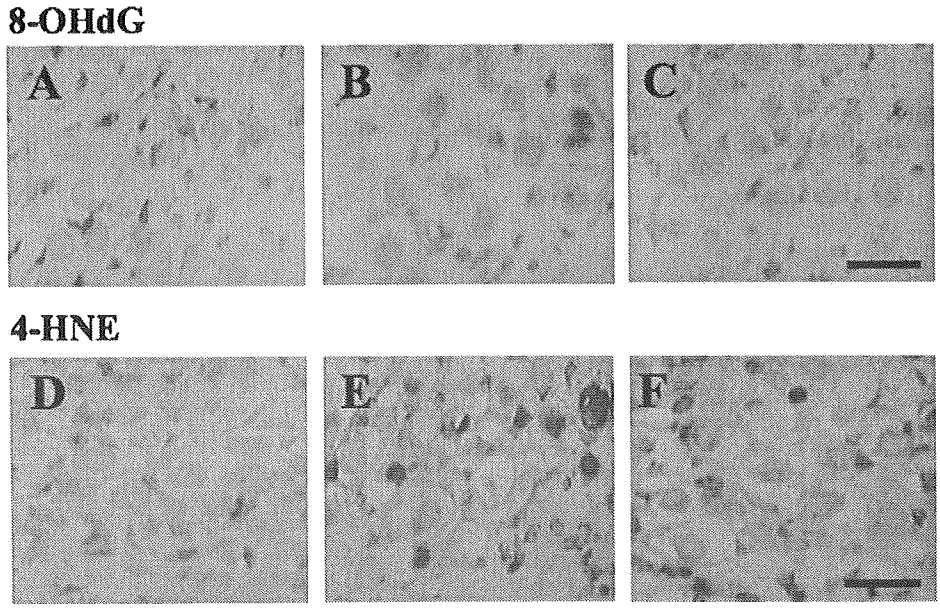


**Fig. 4.** Immunoreactivities of 8-hydroxy-2-deoxyguanosine (8-OHdG) and 4-hydroxy-2-nonenal (4-HNE) in the spiral ganglion cells. Animals for immunohistochemistry of the spiral ganglion cells were sacrificed 1 week after the pressure loading and sections were prepared. Scale bars = 50 μm. (A) Weak immunoreactivities for 8-OHdG were observed in the normal group. (B) Strong immunoreactivities for 8-OHdG were observed in the nuclei of the spiral ganglion cells in the non-treated IEB group. (C) Lesser amounts of immunoreactivity were observed for 8-OHdG in the same region of the edaravone-treated IEB group as compared to that observed in the non-treated IEB group. (D) Weak immunoreactivities for 4-HNE were observed in the normal group. (E) Strong immunoreactivities for 4-HNE were observed in the cytoplasm of the spiral ganglion cells in the non-treated IEB group. (F) Lesser amounts of immunoreactivities were observed for 4-HNE in the same region of the edaravone-treated IEB group as compared to that observed in the non-treated IEB group.

inner ear (Kelemen, 1983). The rupture of Reissner's membrane theory was proposed based on data from an audiogram of an IEB patient. In this patient, the IEB was thought to have induced rupture of Reissner's membrane, which caused a mixing of the endolymph and perilymph that ultimately led to the hearing loss (Simons, 1978). In the round or oval window fistula theory, both the explosive route (cochlear aqueduct and the internal auditory meatus) and the implosive route (eustachian tube and the middle ear) have been suggested as the pathways of the membrane fistula (Goodhill, 1971). The circulatory disturbance theory was based on the autopsy findings of two drowning victims (one from scuba diving and one from a traffic accident) in which there were massive hemorrhages in inner ears that lacked tympanic and round window fistulas (Kelemen, 1983). In the animal model of IEB, scala tympani and scala vestibuli hemorrhages have been previously documented (Tanabe et al., 1986), and in a second study in 180 ears examined after the pressure loading, no fistulas were seen in the round window membranes (Tanabe et al., 1984).

In the present study, cochlea 3 h after the pressure loading showed hemorrhage in the scala tympani, scala media, and scala vestibuli (Fig. 2), indicating that circulatory disturbance plays an important role in IEB's pathophysiology. In another study, free

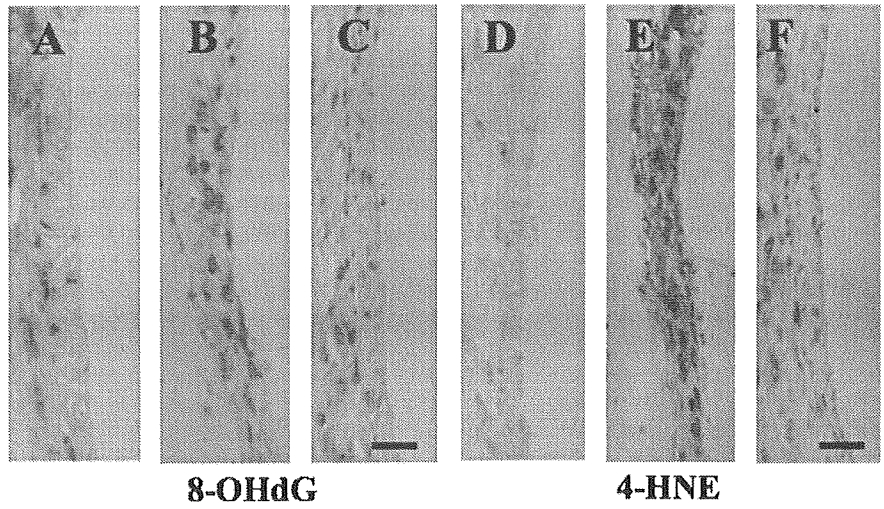


**Fig. 5.** Immunoreactivities of 8-hydroxy-2-deoxyguanosine (8-OHdG) and 4-hydroxy-2-nonenal (4-HNE) in the stria vascularis. Animals for immunohistochemistry of the stria vascularis were sacrificed 1 week after the pressure loading and sections were prepared. Scale bars = 20 μm. (A) Weak immunoreactivities for 8-OHdG were observed in the normal group. (B) Strong immunoreactivities for 8-OHdG were observed in the nuclei of the marginal cells, intermediate cells, and basal cells in the non-treated IEB group. (C) Lesser amounts of immunoreactivity were observed for 8-OHdG in the same region of the edaravone-treated IEB group as compared to that observed in the non-treated IEB group. (D) Weak immunoreactivities for 4-HNE were observed in the normal group. (E) Strong immunoreactivities for 4-HNE were observed in the cytoplasm of the marginal cells, intermediate cells, and basal cells in the non-treated IEB group. (F) Lesser amounts of immunoreactivity were observed for 4-HNE in the same region of the edaravone-treated IEB group as compared to that observed in the non-treated IEB group.

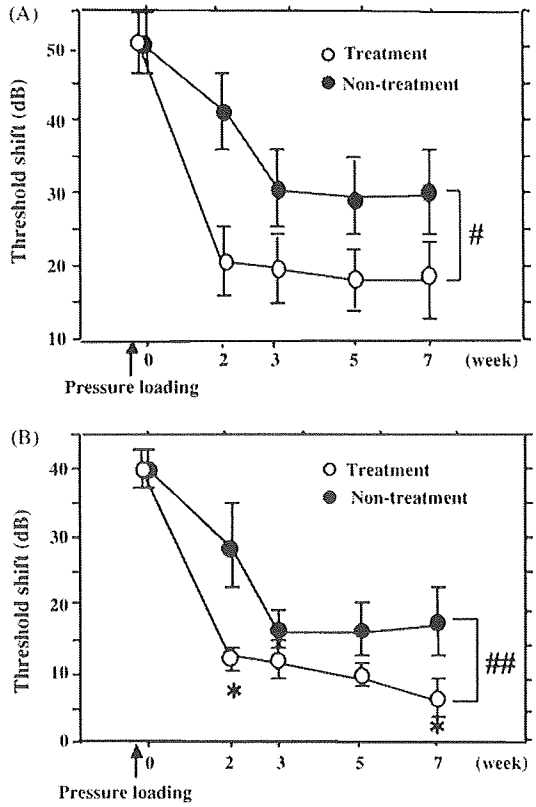


**Fig. 6.** (A) Use of auditory brainstem response (ABR) measurements (30–70 dB) to compare the auditory function between the edaravone-treated ($n = 15$) and the non-treated ($n = 15$) IEB groups. In the ABR measurement, a click at 4 kHz was used for the auditory stimulus followed by the recording of 100 sweeps. As determined by peak I of the waveform, the ABR threshold was recorded from 90 to 20 dB using 10-dB steps. The threshold shift of the edaravone-treated IEB group exhibited significantly faster improvement as compared to that of the non-treated IEB group ($^{\#}P < 0.005$, Repeated Measures ANOVA). There was a marginally significant difference at the final auditory function examination that was performed at 7 weeks after the pressure loading ($P = 0.0564$, Mann–Whitney $U$-test). Values are mean ± SE. (B) Use of ABR measurements (30–50 dB) to compare the auditory function between the edaravone-treated ($n = 9$) and the non-treated ($n = 9$) IEB groups after excluding severely damaged ears (scale out and ≥60 dB were excluded). There was a significantly faster improvement of the threshold shift for the edaravone-treated IEB group as compared to that seen for the non-treated IEB group ($^{\#\#}P < 0.05$, Repeated Measures ANOVA). The significant improvements in the threshold shift in the edaravone-treated IEB group were observed at 2 and 7 weeks after the pressure loading ($^{*}P < 0.05$, Mann–Whitney $U$-test). Values are mean ± SE.

radicals have been demonstrated to be involved in circulatory disturbances of the brain (Demougeot et al., 2004). In the ischemia-reperfusion animal model, hydroxyl radicals (Ohlemiller and Dugan, 1999) and NO (Tabuchi et al., 1999) strongly damaged the cochlea, particularly the OHCs. In the present study, the strong detection of the 8-OhdG immunoreactivity indicated that there was oxidative DNA damage in the OHCs. This suggests that the damage was induced by free radicals that were associated with the IEB. In the present study, obvious hair cell loss was not observed. In the studies on noise-induced hearing loss model, increased ROS activity continues for several days after the intense noise exposure and the persistent ROS activity leads to hair cell death. The mechanism or time course of hair cell damage in IEB might be different from noise-induced hearing loss.

Since our data suggested there was an association between the free radicals and IEB, we hypothesized that the administration of edaravone, which is a free radical scavenger, would be useful as an IEB treatment. In humans, edaravone has been shown to have therapeutic effects on acute brain infarctions (Tohgi et al., 2003) and in acute myocardial infarction (Tsujita et al., 2004). In the inner ear of animals, edaravone has been used to successfully treat endolymphatic hydrops (Takumida et al., 2007). Edaravone inhibits the activation of the lipoxygenase pathway in the arachidonic acid cascade, which in turn prevents the over-production of superoxide anions (Watanabe and Egawa, 1994). It also reacts with hydroxyl or peroxyl radicals to form oxidized compounds in addition to possessing a competitive hydroxyl radical scavenging action (Watanabe et al., 1994).

In the present study, the immunoreactivities of 8-OHdG in the OHCs of the organ of Corti and immunoreactivities of 8-OHdG and 4-HNE in the stria vascularis and spiral ganglion cells were strongly observed in the non-treated IEB group. This suggests that severe pressure changes can cause serious oxidative stress within the cochlear tissue that can ultimately lead to acute SNHL. On the other hand, lesser amounts of immunoreactivity were observed in the inner ear tissue of the edaravone-treated IEB group as compared to that observed in the non-treated IEB group. Weak immunoreactivities were also observed in the inner ear tissue of the normal group. These results indicate that edaravone biochemically reduces the oxidative stress in the cochlear tissue. Functional evaluation by ABR also revealed there was a therapeutic effect of the free radical scavenger on the IEB-induced SNHL. Because the main target of inner ear barotraumas in the present condition was the basal to middle turn, immunoreactivity of 8-OHdG and 4-HNE could be the strongest in the basal turn and less in the apical turn. The different response against IEB among each cochlear turns needs to be further studied.

From the current results, we can infer that the mechanism of pathogenesis of the inner ear barotrauma may be as follows. IEB induces circulatory disturbances that then produce ROS such as hydroxyl radicals. These radicals then damage the organ of Corti, stria vascularis, and spiral ganglion cells, which ultimately causes hearing loss. When edaravone is administered at an early stage of the damage cycle, it is able to remove the cytotoxic radicals, inhibit the oxidative DNA damage, and prevent the lipid peroxidation of the cochlear tissue, so that there is a net improvement of the threshold shift observed. Therefore, the relationship that was observed between ROS and IEB in the current study should have a positive impact on the development of IEB therapies in the future.

In conclusion, the results of the present study indicate that free radicals play important roles in the mechanism of IEB, and that edaravone is therapeutically effective in helping to prevent oxidative damage that can occur as a result of IEB. These findings not only provide a physiological rationale for using edaravone in the clinical treatment of IEB, but also indicate that free radical scavengers might possibly be the therapeutic agent of choice in IEB treatments.

To our knowledge, the present study is the first report to verify that free radicals participate in IEB, and that edaravone is a therapeutically efficacious treatment for IEB.

## Acknowledgements

Edaravone was a kind gift of Mitsubishi Tanabe Pharma Corporation, Osaka, Japan. We are grateful to Dr. Takahiro Nakamura, Laboratory for Mathematics, National Defense Medical College, for his useful advice on statistical discussions.

## References

Demougeot, C., Hoecke, M.V., Bertrand, N., Prigent-Tessier, A., Mossiat, C., Beley, A., Marie, C., 2004. Cytoprotective efficacy an mechanism of the liposoluble iron chelator 2,2′-dipyridyl in the rat photothrombotic ischemic stroke model. J. Pharmacol. Exp. Ther. 311, 1080–1087.

Fetoni, A.R., Sergi, B., Ferraresi, A., Paludetti, G., Troiani, D., 2004. Protective effects of alpha-tocopherol and tiopronin against cisplatin-induced ototoxicity. Acta Otolaryngol. 124, 421–426.

Garetz, S.L., Altschuler, R.A., Schacht, J., 1994. Attenuation of gentamicin ototoxicity by glutathione in the guinea pig in vivo. Hear. Res. 77, 81–87.
Goodhill, V., 1971. Sudden deafness and round window rupture. Laryngoscope 81, 1462–1474.
Goplen, F.K., Gronning, M., Irgens, A., Sundal, E., Nordahl, S.H.G., 2007. Vesitibular symptoms and otoneurological findings in retired offshore divers. Aviat. Space Environ. Med. 78, 414–419.
Kelemen, G., 1983. Temporal bone findings in cases of salt water drowning. Ann. Otol. Rhinol. Laryngol. 92, 134–136.
Maetani, T., Hakuba, N., Taniguchi, M., Hyodo, J., Shimizu, Y., Gyo, K., 2003. Free radical scavenger protects against inner hair cell loss after cochlear ischemia. Neuropreport 14, 1881–1884.
Nakayama, H., Shibayama, M., Yamami, N., Togawa, S., Takahashi, M., Mano, Y., 2003. Decompression sickness and recreational scuba divers. Emerg. Med. J. 20, 332–334.
Ohlemiller, K.K., Dugan, L.L., 1999. Elevation of reactive oxygen species following ischemia-reperfusion in mouse cochlea observed in vivo. Audiol. Neuro-Otol. 4, 219–228.
Parell, G.J., Becker, G.D., 1985. Conservative management of inner ear barotrauma resulting from scuba diving. Otolaryngol. Head Neck Surg. 93, 393–397.
Ryback, L.P., Whitworth, C., Somani, S., 1999. Application of antioxidants and other agents to prevent cisplatin ototoxicity. Laryngoscope 109, 1740–1744.
Schacht, J., 1998. Aminoglycoside ototoxicity: prevention in sight? Otolaryngol. Head Neck Surg. 118, 674–677.
Simmons, F.B., 1978. Fluid dynamics in sudden sensorineural hearing loss. Otolaryngol. Clin. N. Am. 11, 55–61.
Tabuchi, K., Kusakari, J., Ito, Z., Takahashi, K., Wada, T., Hara, A., 1999. Effect of nitric oxide synthase inhibitor on cochlear dysfunction induced by transient local anoxia. Acta Otolaryngol. 119, 179–184.
Takumida, M., Takeda, T., Takeda, S., Kakigi, A., Nakatani, H., Anniko, M., 2007. Protective effect of edaravone against endolymphatic hydrops. Acta Otolaryngol. 127, 1124–1131.
Tanabe, T., Hosokawa, S., Hraide, F., Inouye, T., 1984. Inner ear changes experimentally induced by barotraumas—morphological aspect. Ear Res. Jpn. 15, 228–230.
Tanabe, T., Hosokawa, S., Hiraide, F., Ogura, M., Ohno, H., Inouye, T., 1986. Effect of an earplug on the experimental aural barotrauma. Otologica Fukuoka 32, 481–488.
Tanaka, K., Takemoto, T., Sugahara, K., Okuda, T., Mikuriya, T., Takeno, K., Hashimoto, M., Shimogori, H., Yamashita, H., 2005. Post-exposure administration of edaravone attenuates noise-induced hearing loss. Eur. J. Pharmacol. 522, 116–121.
Tohgi, H., Kogure, K., Hirai, S., Takakura, K., Terashi, A., Gotoh, F., Maruyama, S., Tazaki, Y., Shinohara, Y., Ito, E., Sawada, T., Yamaguchi, T., Kikuchi, H., Kobayashi, S., Fujishima, M., Nakashima, M., 2003. Effect of a novel free radical scavenger, edaravone (MCI-186), on acute brain infarction. Cerebrovasc. Dis. 15, 222–229.
Tsujita, K., Shimomura, H., Kawano, H., Hokamaki, J., Fukuda, M., Yamashita, T., Hida, S., Nakamura, Y., Nagayoshi, Y., Sakamoto, T., Yoshimura, M., Arai, H., Ogawa, H., 2004. Effects of edaravone on reperfusion injury in patients with acute myocardial infarction. Am. J. Cardiol. 94, 481–484.
Watanabe, T., Egawa, M., 1994. Effects of antistroke agent MCI-186 on cerebral arachidonate cascade. J. Pharmacol. Exp. Ther. 271, 1624–1629.
Watanabe, T., Yuki, S., Egawa, M., Nishi, H., 1994. Protective effects of MCI-186 on cerebral ischemia: possible involvement of free radical scavenging and antioxidant actions. J. Pharmacol. Exp. Ther. 268, 1597–1604.
Yamasoba, T., Nuttall, A.L., Harris, C., Raphael, Y., Miller, J.M., 1998. Role of glutathione in protection against noise-induced hearing loss. Brain Res. 784, 82–90.

厚生労働科学研究費補助金
難治性疾患克服研究事業

# 細網異形成症の診断と治療に関する調査研究

## 平成２１年度総括・分担研究報告書

発行日　平成 22 年 3 月 31 日
発行者　野々山　恵章
発行所　厚生労働省難治性疾患克服研究事業
細網異形成症の診断と治療に関する調査研究班
研究代表者　野々山　恵章
〒359-8513
埼玉県所沢市並木３丁目２番地
ＴＥＬ（04）2995-1621
ＦＡＸ（04）2995-5204
印刷所　ニッセイエブロ株式会社
〒105-0004　東京都港区新橋 5-20-4
TEL(03)5733-5151